Old Dominion University
ODU Digital Commons

Physics Faculty Publications | Physics

2010

Excitation-Induced Germanium Quantum Dot Formation on Si (100)-(2×1)

Ali Oguz Er
Old Dominion University

Hani E. Elsayed-Ali
Old Dominion University, helsayed@odu.edu

Follow this and additional works at: https://digitalcommons.odu.edu/physics_fac_pubs

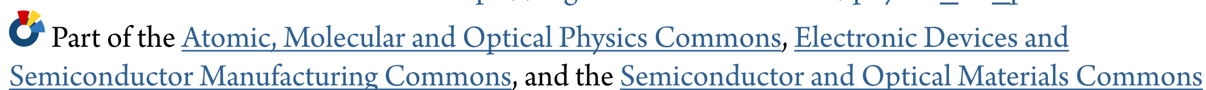
Part of the Atomic, Molecular and Optical Physics Commons, Electronic Devices and Semiconductor Manufacturing Commons, and the Semiconductor and Optical Materials Commons

Repository Citation

Er, Ali Oguz and Elsayed-Ali, Hani E., "Excitation-Induced Germanium Quantum Dot Formation on Si (100)-(2×1)" (2010). *Physics Faculty Publications*. 24.
https://digitalcommons.odu.edu/physics_fac_pubs/24

Original Publication Citation

Er, A. O., & Elsayed-Ali, H. E. (2010). Excitation-induced germanium quantum dot formation on Si (100)-(2×1). *Journal of Applied Physics, 108*(3), 034303. doi:10.1063/1.3462436

This Article is brought to you for free and open access by the Physics at ODU Digital Commons. It has been accepted for inclusion in Physics Faculty Publications by an authorized administrator of ODU Digital Commons. For more information, please contact digitalcommons@odu.edu.

Excitation-induced germanium quantum dot formation on Si(100)-(2×1)

Ali Oguz Er[1] and Hani E. Elsayed-Ali[2,a)]
[1]Department of Physics, Old Dominion University, Norfolk, Virginia 23529, USA
[2]Department of Electrical and Computer Engineering and the Applied Research Center, Old Dominion University, Norfolk, Virginia 23529, USA

(Received 25 March 2010; accepted 11 June 2010; published online 4 August 2010)

The effect of nanosecond pulsed laser excitation on the self-assembly of Ge quantum dots grown by pulsed laser deposition on Si(100)-(2×1) was studied. *In situ* reflection high-energy electron diffraction and *ex situ* atomic force microscopy were used to probe the quantum dot structure and morphology. At room temperature, applying the excitation laser decreased the surface roughness of the grown Ge film. With surface electronic excitation, crystalline Ge quantum dots were formed at 250 °C, a temperature too low for their formation without excitation. At a substrate temperature of 390 °C, electronic excitation during growth was found to improve the quantum dot crystalline quality, change their morphology, and decrease their size distribution almost by half. A purely electronic mechanism of enhanced surface hopping of the Ge adatoms is proposed. © *2010 American Institute of Physics*. [doi:10.1063/1.3462436]

I. INTRODUCTION

While most semiconductor devices are based on silicon, its indirect band gap, and the resulting low probability of radiative transitions, limits its optoelectronics applications. Devices employing Ge/Si epitaxial layers can overcome this restriction.[1] For example; a dense array of small, narrow size distribution Ge islands embedded in Si layers can be used for light emission where electron hole pairs are captured in the Ge islands. Growth of Ge on Si is a classical model of the Stranski–Krastanov growth-mode, also known as layer-plus-island growth, where growth starts in a uniform layer-by-layer growth up to ~3 monolayer (ML). [1 ML is equivalent to 6.78×10^{14} atoms/cm^2 on a Si(100) surface.] The lattice mismatch (misfit) between Ge and Si ($a_{Ge}=0.566$ nm and $a_{Si}=0.543$ nm) causes elastic strain which increases as the Ge film grows on the Si surface. With the increase in strain energy, the competition between chemical potential of the deposited film and strain energy eventually causes the film to continue through three-dimensional (3D) island growth beyond a critical layer thickness around 3 ML. The value of the misfit is the key factor for the relief mechanism. Three dimensional island formation leads to a partial relaxation of strain. Those islands could be dislocation free or coherent and their shapes change during growth.

Pulsed laser-induced electronic processes leading to surface structural modifications have been shown to occur when the laser intensity is below the melt threshold.[2–5] Recent scanning tunneling microscopy studies have demonstrated that laser pulses well below the melt and ablation thresholds induce bond rupture at individual atomic sites on several semiconductor surfaces via a process that is purely electronic.[6–8] The laser-induced electronic bond rupture causes structural changes on the surface which depend strongly on the surface studied.

Low temperature thin film growth is strongly desirable in microelectronic fabrication. In Si/Ge, it has been long recognized that one way to suppress misfit dislocations is by lowering the growth temperature.[9] To lower the epitaxial growth temperature, extrinsic assistance by energetic particles, such as ions, electrons, and photons have been used to add energy to promote the migration of adsorbed atoms at the surface.[10–12]

Treatment of silicon surfaces by a Nd-doped yttrium aluminum garnet (Nd:YAG) laser was used to improve surface wettability and adhesion characteristics.[13] Also, illumination of silica substrates with a very low intensity diode laser during deposition was reported to unify the clusters' shapes and narrow the size distribution of Ga nanoparticles grown at ~100 °C.[14] Moreover, irradiation by a few hundred eV electron beam during deposition of CeO_2 on Si was reported to enhance surface epitaxy by reducing the required temperature for epitaxial growth from 820 to 710 °C.[10] In another work, a low-energy electron beam was used to modify the surface and achieve high quality GaAs film grown on an insulator on silicon.[12] Pulsed ion-beam irradiation during heteroepitaxy of Ge on Si led to modifying the average size and size distribution of Ge islands grown by molecular beam epitaxy (MBE).[15] Postdeposition nanosecond pulsed laser treatment of Ge quantum dots (QDs) grown on Si reduced the QD surface density, modified their composition, and increased their average size, making the QD size more uniform after the treatment.[16] Nonthermal laser-induced desorption has also been widely studied for different metals and semiconductors.[17–19]

We have recently studied the effects of nanosecond pulsed laser-induced electronic excitations on the self-assembly of Ge QD on Si(100)-(2×1) grown by pulsed laser deposition (PLD).[20] Electronic excitations, due to laser irradiation of the Si substrate and the Ge film during growth, were shown to decrease the roughness of films grown at a substrate temperature of ~120 °C. At this temperature, the grown films showed no long-range order as detected by reflection high-energy electron diffraction (RHEED). Elec-

a)Electronic mail: helsayed@odu.edu.

 © 2010 American Institute of Physics

tronic excitation resulted in the formation of an epitaxial wetting layer and crystalline Ge QD at ~260 °C, a temperature at which no crystalline QD formed without excitation under the same deposition conditions. Here we expand the scope of this work by studying excitation effect on deposition at various substrate temperatures and excitation with different laser energy densities. The effect of applying the excitation laser on the growth morphology is studied. It is shown that the excitation laser affects the morphology only when applied during growth with no postdeposition annealing effects observed at the studied laser energy densities. The results are consistent with an electronically driven mechanism that increases surface diffusion of the incoming Ge flux.

II. EXPERIMENT

Ge QDs were grown in an ultrahigh vacuum (UHV) chamber ($\sim 1\times 10^{-9}$ Torr) by PLD. The Ge target was mounted on a rotation stage with a variable rotation speed. Target rotation at 5 rpm was used to minimize the particulate formation during deposition. The laser beam profile on target and target rotation speed were set such that the spatial separation of the laser pulse spots on target were ~0.6 of its full width at half-maximum (FWHM), resulting in ablation of the target surface by no more than two laser pulses. The Si(100) substrates (dimensions of $2.0\times 10\times 0.5$ mm^3 *p*-type boron doped and resistivity 0.060–0.075 Ω cm, miscut angle 0.38°) were chemically etched by using a modified Shiraki method before being loaded into the UHV chamber. The Ge target was a 2″ disk, 0.5 mm thick, undoped *n*-type, with a resistivity of 45–58.7 Ω cm. The vacuum system was then pumped down, baked more than 24 h and, finally, cooled down to room temperature. The Si(100) sample was degassed at ~700 °C for another 24 h and then flashed to ~1200 °C for ~60 s to obtain the (2×1) reconstruction. The substrates were heated by direct current flow. The surface temperature was initially measured using a combination of a chromel-alumel (K-type) thermocouple that was mechanically attached to the substrate surface and a Mikron MI-GA15 pyrometer. The thermocouple was used for temperature measurement up to ~400 °C, while the pyrometer was used for higher temperatures. The thermocouple calibration was checked, before installing it into the UHV chamber, using the boiling point temperature of water. A temperature calibration curve relating the surface temperature obtained by the K-type thermocouple and the pyrometer to the sample conductivity was obtained and used for subsequent temperature measurements. This approach was used to avoid complications due to changes in thermocouple properties by repeated flashing at high temperatures. We can measure temperature reproducibly and with an accuracy of ±17 °C, mainly limited by the accuracy of determining sample conductivity with temperature.

A Q-switched Nd:YAG (wavelength $\lambda=1064$ nm, FWHM of ~40 ns, 10 Hz repetition rate) was split into an ablation beam and an excitation beam of nonequal powers by means of a half wave-plate and a thin film polarizing beam splitter. The *p*-polarized ablation beam was focused on the rotating Ge target to a spot size ~400 μm (measured at 1/e of the peak value), resulting in a laser energy density of ~5 J/cm^2. The *s*-polarized excitation beam was left unfocused with a beam diameter of ~6.0 mm (measured at 1/e peak value) and was used to irradiate the sample surface. Both the ablation and the excitation laser beams were incident on the Ge target and Si substrate at 45°. A 20 keV well-collimated RHEED electron gun with a spot size less than 90 μm diameter was used to monitor the growth dynamics, while a partially coated phosphor screen displayed the electron diffraction pattern, which was recorded by means of charge-coupled device camera. The electron beam had a grazing angle ~3° with the Si(100) surface. Sample-to-target distance was ~8 cm. The final film thickness measurement was done by a spectroscopic ellipsometer (Woollam M44). Postdeposition tapping-mode atomic force microscope (AFM) was used to study the morphology of the film. The Ge films were grown on Si(100)-(2×1) at different substrate temperatures and different laser excitation energies. The growth dynamics and morphology of the films grown under the laser excitation are compared to those grown at the same deposition conditions without excitation laser.

III. RESULTS AND DISCUSSIONS

A. Results

1. Deposition at 390 °C

The effect of laser excitation of the substrate for Ge growth on Si(100)-(2×1) was studied for a substrate temperature of 390 °C. The Ge was deposited at a rate of ~0.03 ML/s (~0.003 ML/pulse). The deposition rate was obtained from the final Ge thickness using an ellipsometer. The ablation laser energy density was ~5 J/cm^2. Figure 1(a) shows a series of RHEED patterns taken for different Ge coverage without applying any laser substrate excitation. Before deposition, a clean reconstructed Si(100)-(2×1) is observed. The RHEED pattern consists of sharp spots aligned on Laue circles. The diffraction pattern features remain unchanged during the initial stage of deposition, corresponding to the epitaxial growth of the wetting layer (~3 ML) and then become elongated streaks, resulting from deposition of Ge atoms making the surface rougher. The RHEED pattern obtained at ~12 ML coverage shows elongated transmission patterns. After ~15 ML coverage, the streak intensity is reduced. As the deposition further progresses, the surface topography changes and the elongated spots become shorter. Rounded diffraction spots are observed and additional transmission spots appear in the RHEED pattern after ~20 ML coverage. If the deposition is further extended, a rounded, intense transmission pattern develops at ~22 ML coverage. Rounded spots not falling on Laue circles result from transmission of electrons through faceted islands. The AFM image in Fig. 1(b), taken after deposition of ~22 ML, shows well distributed islands with different sizes and shapes. The majority of those islands in this sample are rectangular-based huts and square-based pyramidal shape. The sharp RHEED spots reveal the crystalline nature of these islands. The island density is 5.0×10^9 cm^{-2} and the coverage ratio is 14.5%.

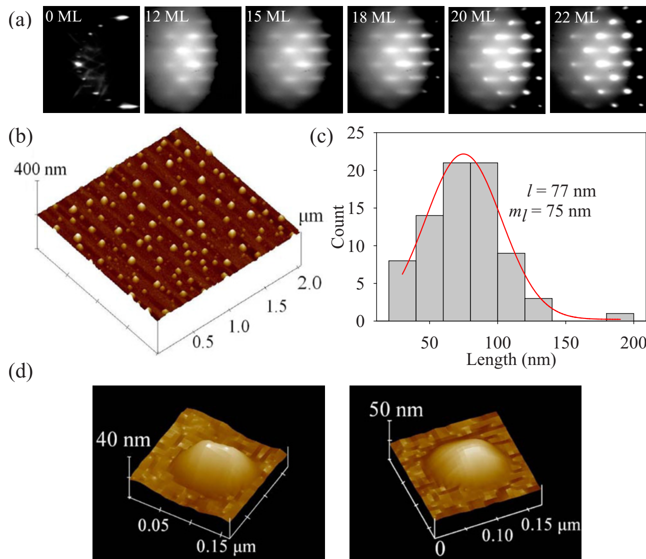

FIG. 1. (Color online) (a) RHEED pattern at different deposition times for a substrate temperature of 390 °C. 20 keV electron beam energy, angle of incidence with the surface ~2.5 ± 0.4° and ablation laser energy density of 5 J/cm^2 is used in all experiments unless otherwise stated. (b) AFM image shows well distributed islands with different sizes and shapes. The majority of those islands are rectangular-based huts and square-based pyramidal shape island. (c) Size distribution shows average length l=77 nm and the most expected length, m_l=75 nm. (d) Individual islands.

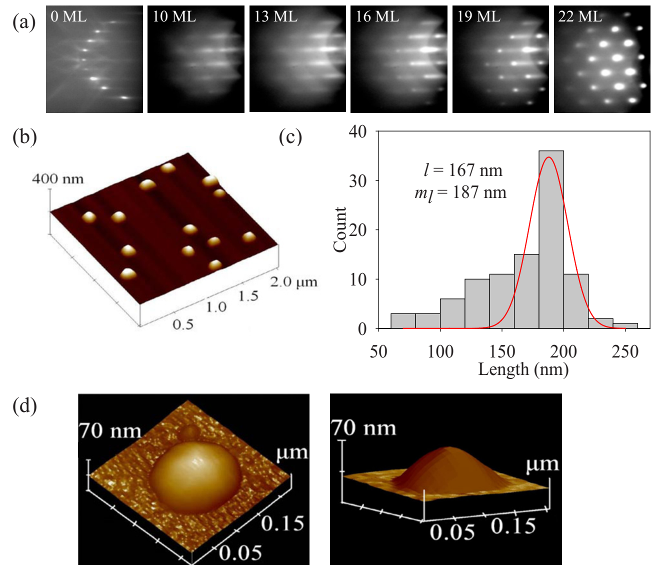

FIG. 2. (Color online) (a) RHEED pattern obtained at different deposition times. Excitation laser energy density = 106 ± 10 mJ/cm^2. (b) AFM image. (c) Island size distribution. With the excitation laser, the islands become more rounded and they lose their facetation. Island density, coverage ratio, and variation in size, area and height decrease, while average length, height, and area increase when the excitation laser is used. Average length l and most expected length m_l are 167 nm and 187 nm, respectively. (d) Individual dome-shaped islands and square-based pyramids are seen in AFM images.

Figure 1(c) shows that the average island length l, measured along the major axis, is 77 nm, and the most expected length m_l is 75 nm. The FWHM of the size distribution is ~80 nm. The average diameter and average height are 51 nm and 15 nm, respectively (height-to-base diameter ratio ~0.3). The variation in the aspect ratio β, defined as height/lateral size, in these islands is 20%. Examples of rectangular-based huts and square-based pyramidal islands can be seen in Fig. 1(d).

The growth of Ge QDs on Si(100) was then studied while applying an excitation laser to the substrate. Figure 2(a) shows RHEED patterns obtained during growth of Ge on Si(100) while an excitation laser with an energy density of 106 ± 10 mJ/cm^2 is applied to the substrate. The Si(100)-(2×1) reconstruction is visible before deposition. One may notice that the initial RHEED pattern of the (2 ×1) reconstructed substrate looks slightly different when comparing Fig. 1(a) with Fig. 2(a) due to slight differences in the electron angle of incidence, how much of the electron beam is intercepted by the sample, and day-to-day variations in the electron beam incidence azimuth and beam quality. All depositions were done on (2×1) reconstructed substrates and the results were not sensitive to these variations in the initial RHEED pattern of the substrate. An elongated RHEED streak pattern is observed at Ge coverage of ~10 ML. As the Ge coverage increases, the intensity of the streaks increases, as shown in the RHEED pattern taken at ~13 ML. Round spotty RHEED patterns start to appear after ~16 ML coverage. At ~19 ML, the elongated streaks become faint and rounded in shape, indicative of the new facet formation in the grown domes. The RHEED pattern shows well defined transmission features with sharp spots after ~22 ML. With the use of the excitation laser at a substrate temperature of 390 °C, the Ge coverage that causes the formation of a transmission pattern becomes larger than without excitation. The corresponding AFM image in Fig. 2(b) shows that the film morphology consists of mainly multifaceted dome-shaped islands coexisting with a small fraction of square-based pyramids. Those islands have a narrow size distribution, as shown in Fig. 2(c). With laser substrate excitation, the island density reduces by a factor of 10 to ~4.7×10^{8} cm^{-2}, and the coverage ratio decreases to 8.0%. Average height of the islands is 35 nm but some of them can reach up to 56 nm. The mean diameter of those islands is ~139 nm, giving rise to a height-to-base ratio ~0.25. Average island length l is ~167 nm, while the most expected length m_l is 187 nm, as shown in Fig. 2(c). The FWHM of the size distribution graph decreased to 45 nm compared to that without laser excitation shown in Fig. 1(c). The variation in the aspect ratio β in these square-based domes is 12%. At a substrate temperature of 390 °C, the island morphology changes when irradiating the silicon surface with the excitation laser. The rectangular-based huts and square-based pyramids transform into dome-shaped islands. Island density, coverage ratio, and variation in size, area, and height decrease, while average length, height, and area increases. Examples of dome-shaped islands and square-based pyramids are shown in Fig. 2(d).

2. Deposition at 250 °C

The effect of the excitation laser on the Ge growth on Si(100)-(2×1) at a substrate temperature of ~250 °C was also studied. For samples grown below 390 °C, the intensity of the Si(100)-(2×1) RHEED spots decay continuously with deposition time until they disappear, resulting in a diffuse pattern. This indicates the formation of 3D structures

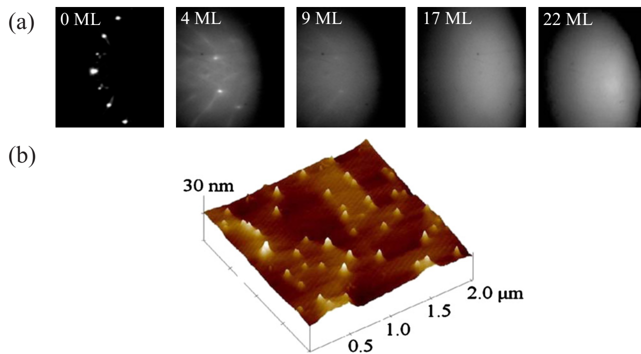

FIG. 3. (Color online) (a) For deposition at 250 °C without an excitation laser, the RHEED pattern decays continuously with coverage resulting in a diffuse pattern. (b) AFM image could be described as a collection of 3D clusters with different shapes and sizes.

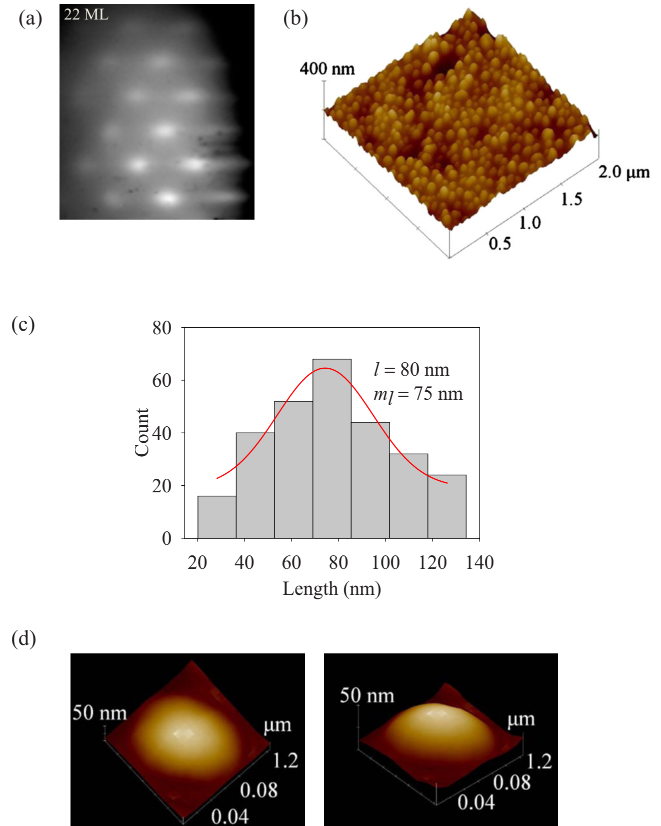

FIG. 4. (Color online) (a) RHEED pattern of 22 ML Ge deposited at 250 °C with an excitation laser of 37 ± 4 mJ/cm^2 shows a transmission pattern. (b) AFM image of the surface shows high-density Ge islands with a majority of rectangular-based huts. (c) Size histogram from the AFM image shows that the average length l and the most expected length m_l are 80 nm and 75 nm, respectively. (d) AFM images of individual islands.

that collectively lack long-range order, as was confirmed by RHEED and AFM measurements. The Ge growth was observed at 250 °C with an ablation laser energy density of 5 J/cm^2 without excitation laser. For RHEED patterns in Fig. 3(a), some of the diffraction patterns remained while others were lost after depositing at ~4 ML. Almost no pattern appeared after 9 ML, which indicated loss of long-range order on the surface. The AFM image obtained after 22 ML, shown in Fig. 3(b), could be described as a collection of 3D clusters with different shapes and sizes. This type of AFM image is generally observed for heteroepitaxy at low temperatures.

Three different laser energy densities were used to study the excitation laser effect at 250 °C. The ablation laser energy density was kept at 5 J/cm^2, while the excitation laser energy density was varied. For an excitation laser energy density of 37 ± 4 mJ/cm^2, the RHEED image in Fig. 4(a), taken 22 ML Ge coverage, shows a spotty transmission pattern, indicating 3D growth. The AFM image in Fig. 4(b) shows high-density of Ge islands, most of which are rectangular-based huts. The density of islands is $\sim6.7\times10^9$ cm^{-2} with a coverage ratio of 24%. Average length l and the most expected length m_l are 80 nm and 75 nm, respectively, as shown in Fig. 4(c). The average height is ~21 nm and average base diameter is 87 nm, giving a height-to-base diameter ratio of ~0.24. AFM images of two of these islands are shown in Fig. 4(d).

Next, the excitation laser was increased to 77 ± 7 mJ/cm^2, while maintaining the ablation laser energy density at 5 J/cm^2 and the substrate temperature at 250 °C. The RHEED pattern after 22 ML Ge coverage, shown in Fig. 5(a), does not change significantly from that in Fig. 4(a). However, the island density and coverage ratio decreased, while the mean area and length increased, as shown by comparing the AFM image of Fig. 5(b) with that in Fig. 4(b). In Fig. 5(b), Ge islands with different shapes and sizes are visible. Those islands are mainly consisting of rectangular-based huts and some small fraction of square-based pyramids. The average island size increases at this laser energy density when compared to conditions used in Fig. 4(b). This may be due to coalescence of the small islands to larger ones. Island density decreases to 3.0×10^9 cm^{-2} and the coverage ratio also decreases to 14%. Figure 5(c) shows that the average length also increases to 94 nm and the most expected length at this condition becomes ~100 nm. The average height is ~23 nm and average base diameter is ~91 nm giving a height-to-base diameter ratio of ~0.25. Figure 5(d) shows AFM images of two of these islands.

The excitation laser density was finally increased to 106 ± 10 mJ/cm^2 while the substrate temperature was kept at 250 °C. Figure 6(a) shows RHEED patterns obtained at different Ge coverage. A clean, reconstructed Si(100)-(2×1) surface is obtained prior to Ge deposition. After ~10 ML, elongated streaks appear, while the first rounded pattern forms at ~15 ML. The intensity of the RHEED diffraction streaks decreases with coverage and those elongated streaks almost disappear at ~19 ML, while round transmission features become strong. Two more transmission features appear after depositing ~21 ML, indicative of the formation of new facets as the islands grow. AFM images and its size distribution for this sample after 22 ML coverage are shown in Figs. 6(b) and 6(c). Three distinctive island shapes are observed. These are rectangular-based huts, square-based pyramids, and some multifaceted domes, shown in Fig. 6(d). Comparing the Ge island morphology at these conditions to that obtained at the lower excitation laser energy density shows a decrease in island density and an increase in the average area and length as the laser energy density is increased. For an excitation energy density of

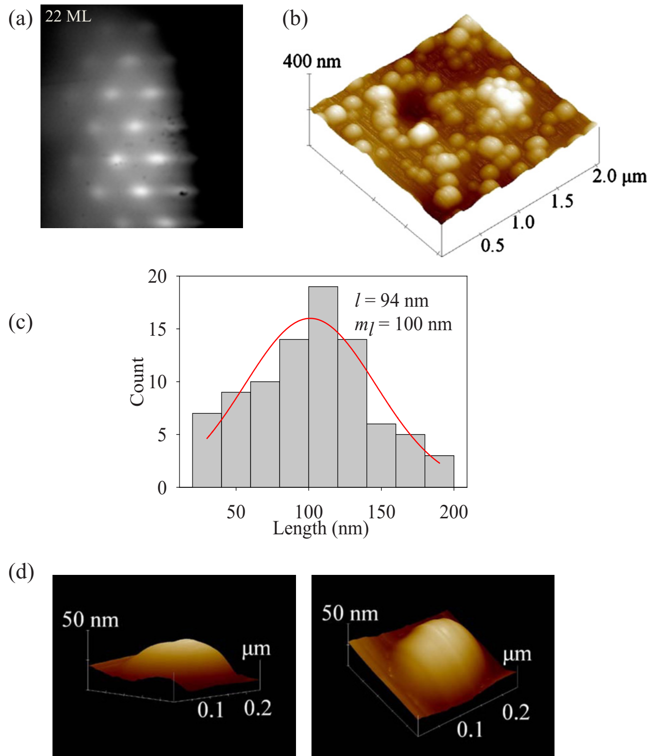

FIG. 5. (Color online) (a) RHEED pattern of 22 ML Ge deposited at 250 °C with an excitation laser of 77 ± 7 mJ/cm^2. (b) AFM image of the surface. (c) Size histogram from the AFM image shows that the average length l and the most expected length m_l are 94 nm and 100 nm, respectively. (d) AFM images of individual islands.

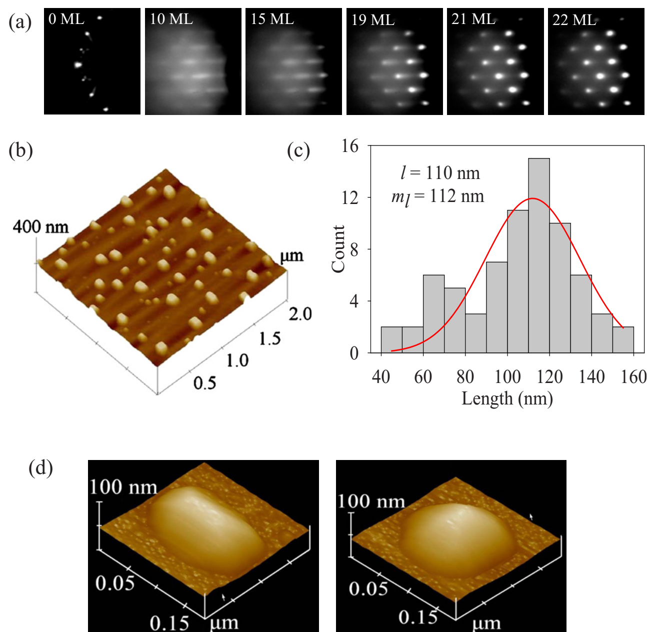

FIG. 6. (Color online) (a) RHEED patterns recorded at different Ge coverage deposited at 250 °C with an ablation laser of 5 J/cm^2 and an excitation laser of 106 ± 10 mJ/cm^2. (b) AFM image of the final 22 ML Ge film shows that film is consisting of rectangular-based huts, square-based pyramids along with some multifaceted domes. (c) Size histogram of the AFM image shows that the average length l and the most expected length m_l are 110 nm and 112 nm, respectively. (d) AFM images of some of the individual islands show rectangular-based huts, square-based pyramids, and some multifaceted domes.

106 ± 10 mJ/cm^2, the island density is $\sim1.4\times10^9$ cm^{-2}, coverage ratio 11%, with average island length 110 nm and most expected length 112 nm, as shown in the island size distribution in Fig 6(c). The average height is ~27 and average base diameter is ~113 nm, giving rise to height-to-base diameter ratio ~0.24. The variation in the aspect ratio of the clusters is 23%. The larger island sizes observed here compared to that in Ref. 20 is mainly due to the increases Ge film thickness. Also, in the present study the laser repetition rate was 10 Hz compared to the previously used 50 Hz.[20] Higher pulse repletion rate in PLD reduces surface relaxation between pulses causing agglomeration.

Increasing the excitation laser energy from 37 ± 4 to 106 ± 10 mJ/cm^2 for a substrate temperature of 250 °C causes island density and coverage ratio to decrease, while the average area, length, and height of the islands increase and size distribution become narrower when the highest excitation laser energy density is used at this temperature. With the increase in the excitation energy density, the Ge islands become more uniform in size and shape. Their height-to-base diameter ratio remains unchanged as the excitation laser energy density is increased. The island densities obtained in the present experiments are smaller than those obtained in other growth techniques. Island densities varied from 10^9 to 10^{11} cm^{-2} in MBE and chemical vapor deposition.[21,22] This may be due to the low deposition rate used. Diffusion length L can be expressed as $L=(Dt)^{1/2}$, where D is the coefficient of adatoms and t is the diffusion time. A higher deposition rate could lead to shorter t, due to competing interactions among the deposited atoms, giving rise to smaller diffusion length. Thus, smaller growth rates produce a smaller density of islands when compared to higher growth rates.

In all the present studies, 1064 nm laser pulses were used with the p-polarized light used for target ablation while s-polarized light used for excitation of the substrate. Both ablation and excitation beams were incident 45° on the surface of the target and substrate, respectively. It is known that s-polarized light couples less to Ge and Si than p-polarized light.[23] It was previously shown that surface vacancies were not formed when the surface was irradiated by laser pulses of 80 fs duration at 2200 nm polarized perpendicular to the Si(111)-(2×1) chain direction. This particular Si surface shows a strong surface transition around 0.45 eV.[24] We are not aware of any Si(100) or Ge surface specific transitions that couple to 1064 nm laser pulses. Therefore, it is reasonable to expect that the laser polarization only affects energy coupling to the surface.

3. Deposition at room temperature

The effect of the excitation laser was also studied for Ge growth on Si(100)-(2×1) at room temperature. Figure 7(a) shows RHEED patterns taken during growth without laser excitation, while in Fig. 7(b) an excitation laser energy density of 106 ± 10 mJ/cm^2 was applied. Without laser excitation the RHEED pattern almost disappeared at Ge coverage of ~9 ML, while with laser excitation some diffraction spots are visible even after 22 ML coverage. In Fig. 7, an ablation laser energy density of 5 J/cm^2 was used without and with laser excitation. All other experimental conditions,

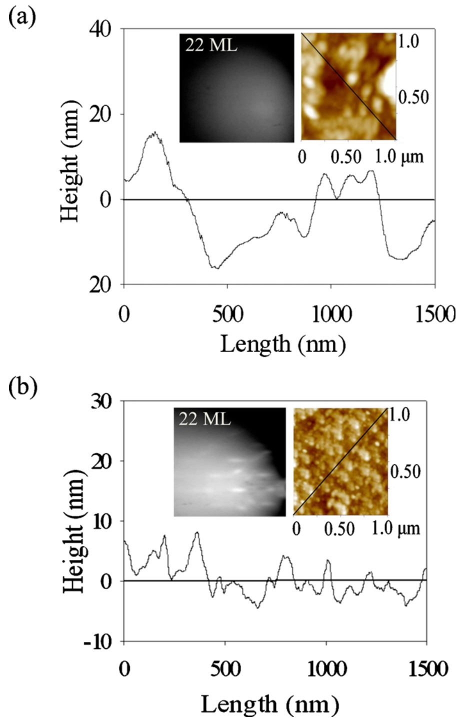

FIG. 7. (Color online) (a) RHEED patterns recorded at different Ge coverage deposited at room temperature with an ablation laser energy density of 5 J/cm^2 and corresponding AFM image of the final 22 ML Ge film. The line scan across the AFM image shows mean surface roughness is 8.6 nm without excitation laser. (b) RHEED patterns and AFM image for the same conditions as in (a) but with an excitation laser energy density of 106 ± 10 mJ/cm^2 showing decrease in surface roughness when the excitation laser is used.

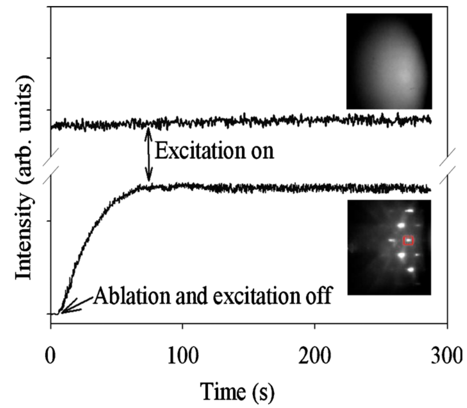

FIG. 8. (Color online) Intensity of the specular spot after termination of Ge deposition with the substrate maintained at 250 °C for a Ge coverage of ~22 ML. In the bottom scan, both the ablation laser (fluence 5 J/cm^2) and the excitation laser (106 ± 10 mJ/cm^2) were turned off at time t=0. The excitation laser was then turned on at t=75 s. In the top scan, no excitation laser was used. The ablation laser was turned off at t=0 s.

such as laser repetition rate, target rotation speed, and target-to-substrate distance, remained the same for Figs. 7(a) and 7(b). Hegazy and Elsayed-Ali[20] previously observed that the deposition time required for the RHEED pattern to disappear when the excitation laser was used was nine times longer than without excitation laser when the substrate was kept at 120 °C. The decay in the RHEED elastic diffraction intensity (Bragg peaks) and the increase in the inelastic background are associated with increased film roughness with deposition. For the substrate kept at room temperature, applying the excitation laser to the substrate during growth decreases the surface roughness, although epitaxial growth was not achieved. AFM images and single-line scans of surface topography can be seen in Fig. 7(a) for the sample grown without excitation laser and in Fig. 7(b) for the sample irradiated with laser. Mean surface roughness of the sample grown at room temperature without excitation laser was found to be 8.6 nm, whereas, with laser excitation the mean surface roughness was 2.1 nm.

The possibility of altering the surface properties by postdeposition laser irradiation was tested. Figure 8 shows the intensity of the RHEED specular spot after termination of Ge deposition with the substrate maintained at 250 °C for Ge coverage of ~22 ML. In the bottom scan, both the ablation laser (energy density 5 J/cm^2) and the excitation laser (106 ± 10 mJ/cm^2) were turned off at time t=0. In this case, the film had grown epitaxially due to the presence of the excitation laser. Upon growth termination, the RHEED intensity showed the usual recovery in a time that depends on surface diffusion. We then only turned on the excitation laser at t=75 s. The intensity of the specular beam did not change, thus, showing no surface annealing by postdeposition application of the excitation laser. In the top scan, we only used the same ablation laser fluence also at a substrate temperature of 250 °C to deposit ~22 ML Ge. No excitation laser was used in this case. The ablation laser was turned off at t=0 s. In this case, the Ge film grew as a rough, disordered surface that only showed a RHEED background with no visible diffraction orders. The intensity reported in Fig. 8 was that of the background that developed in the same location of the specular spot. We did not observe any changes in this intensity, which shows that the postdeposition surface excitation does not result in surface annealing.

B. Discussions

The results show that irradiation of the substrate by the excitation laser has an effect on Ge growth similar to that observed when the substrate temperature is raised. Basically, there appears to be a mechanism driven by the excitation laser that results in enhanced Ge adatom surface diffusion. The thickness measurement was performed using an ellipsometer. For samples without laser excitation, the Ge thickness measured after 8000 pulses was 32.5 ± 1.5 Å, while with excitation the Ge thickness was 33.7 ± 1.0 Å. Therefore, within the experimental error, there appears to be no effect on Ge film thickness due to the excitation laser, and any atom desorption by electronic excitation is too small to affect the grown film.

When the sample is irradiated by the pulsed laser, the initial effect is to generate electron-hole pairs. The bulk silicon is known to have an indirect band gap of 1.12 eV. Optical measurements show that the Si(100) surface has also an indirect band gap of 0.44–0.64 eV.[25,26] Although the Si(100)-(2×1) surface has surface specific optical transitions, their contribution is small for excitation with 1064 nm wavelength.[7] Due to the low surface absorption coefficient ($\alpha = 11$ cm^{-1}) of the 1064 nm radiation in Si, photoexcitation

takes place mainly in the bulk. Therefore, the primary effect of the 1064 nm nanosecond laser light on the Si substrate is bulk-valence excitation to generate holes and electrons with small excess energies.[27] The energy density of the ns laser pulses used are well below the melt threshold of Si.[28] We next discuss thermal and nonthermal (electronic) effects of the excitation laser on Ge QD growth.

1. Thermal effects

The surface temperature rise due to laser heating is calculated using a one-dimensional, heat diffusion model. According to this model, the maximum temperature rise due to absorption of the 1064 nm excitation laser in the skin depth of Si ($\sim 60\ \mu m$) is $\sim 23\ °C$. The surface temperature drops to the substrate temperature by heat diffusion in $\sim 0.1\ \mu s$. For Ge, the skin depth for 1064 nm is 200 nm, and the maximum temperature rise in this case is $\sim 200\ °C$ if irradiated with $106 \pm 10\ mJ/cm^2$, which is the maximum laser energy density used during the present work. Heat diffusion to the Si substrate limits the temperature excursion time to $<0.1\ \mu s$. The macroscopic diffusion of Ge atoms adsorbed on the Si(100)-(2×1) surface has been shown to follow the Arrhenius behavior:[29] $D = D_0 \exp(-E_T/kT)$, where $D_o = 4.3 \times 10^{-4}\ cm^2/s$ is a pre-exponential constant, $E_T = 1.17\ eV$ is the activation energy, and k and T are the Boltzmann's constant and temperature, respectively. The Ge atoms move just $\sim 1.6 \times 10^{-11}\ cm$ in 100 ns at 250 °C, which is clearly too small to affect the nucleation and growth mechanism. Therefore, we can exclude laser heating as a possible mechanism affecting Ge growth morphology due to the short temperature excursion time and small temperature rise.

2. Nonthermal effects

Energy transfer from laser generated hot electrons to surface adatoms has been reported to improve the crystalline quality.[10] The important role of hot electrons has been demonstrated in the study of molecular desorption from metal surfaces under fs-laser excitation that can result in high effective electron temperature.[30] However, the photon energy of 1064 nm light is $\sim 0.05\ eV$ above the silicon band gap energy, resulting in low free-carrier energy.[31] Thus, for single-photon absorption by bound carriers in Si, the role of hot carriers in increasing surface vibrations is expected to be negligible. Moreover, because of the low intensity of the excitation laser and relatively low substrate temperature, free carrier and two-photon absorption are negligible for conditions considered in the present work.[31,32] The band gap of Ge is 0.66 eV; thus, the excitation photon energy is $\sim 0.5\ eV$ above the Ge band gap and, therefore, has enough energy to cause surface modification by electronic excitation.

It is well known that an electron or a photon interacting with the surface can induce an electronic excitation. Emission of ions or neutral particles due to this excitation can occur. Such processes are called desorption induced by electronic transitions (DIETs).[33] Two established DIET mechanisms are the Knotek–Feibelman (KF) model and the Menzel, Gomer, and Redhead (MGR) model.

Knotek and Feibelman[34] studied the mechanism of electron stimulated desorption of positive ions from certain d-band metal oxides. This mechanism requires initial core-hole creation, followed by the production of two holes via Auger decay and, finally, coulomb repulsion between this positive ion and the cation leads to the emission of a positive ion from the surface. The KF mechanism requires electrons or photons with energies of tens of electron volt and, therefore, this mechanism can be ruled out in the present study based on the relatively low photon energy used.[19]

A more general model of DIET is the MGR model that explains the electron desorption due to energy excitation from a bonding to an antibonding electronic state.[35,36] In this model, an excitation causes a Franck–Condon transition where the electronic transition occurs without changes in the positions and momentum of the nuclei. It is assumed that the initial excitation occurs by absorption of a photon or electron to a repulsive excited state. This excitation accelerates the adsorbate away from the surface, converting potential energy into kinetic energy of the adsorbate before quenching to the ground state. Depending on how long the adsorbate was accelerated on the repulsive state, this may cause it to overcome the desorption barriers for neutral or atomic species. Because the photon energy in the present study is only $\sim 0.05\ eV$ above the Si band gap, the electronic transition probability for DIET, as described by the MGR model, will be too small to cause any desorption or significant vibrational excitation at the Si surface.[35] Even for Ge, the 0.5 eV excess energy is relatively low compared to surface atom binding energies.[37] Also, the MGR model treats the interaction between light and matter as an isolated event. Since excitons on silicon and also germanium surfaces are not self trapped and the applied photon energy is relatively low, the MGR model for desorption does not appear to be likely for the conditions used in our experiment.[38]

In another model, Sumi proposed two-hole localization (THL) and applied his model successfully to explain electronically induced bond rupture at Si and other surfaces.[6,39–41] The primary assumption in THL is that surface bond rupture leading to neutral-atomic desorption can be induced by strong lattice relaxations associated with localization of two valence holes on the same surface bond. This assumption is based on the Anderson negative U concept suggesting that THL can occur if the Coulomb repulsion energy $E_{Coulomb}$, due to on-site localization of carriers with same charge, is smaller than the lattice relaxation energy E_{LR} which comes from the lattice distortion and polarization on the localizing particle.[42]

THL on surface sites of nonequilibrated valence holes was concluded to be the mechanism responsible for bond breaking when a Si(111)-(2×1) surface was excited by 1064 nm, 3.5 ns laser pulses.[39] Surface bond rupture rate was studied for Si(111),[3,7,24,39] Si(100),[41,43,44] and other materials.[3] The rate of bond rupture varies between 3×10^{-5} and 8×10^{-10} ML/pulse depending on the laser wavelength and fluence. The minimum desorption rate in those studies is $\sim 10^{-5}$ ML/pulse, although the wavelength 1064 nm was found to be inefficient to induce desorption from the Si(100)-(2×1) surface.[41]

THL at a surface site affects the surface atom bonding weakening the bond and inducing a strong atom vibration. The localization of the second hole causes strong vibrations of the surface atom, which could lead to bond breaking. These atoms could be ejected due to this transient strong lattice vibration (phonon-kick) with a distribution of translational energies that starts from a given onset.[5] Vibrational relaxation after electronic excitation would lead to many phonons being emitted. The lattice forms a continuum of motions that can absorb the energy of the vibrational relaxation. As the energy of the surface atoms increases, the bonded atoms vibrate more strongly. If the phonon-kick perpendicular to the surface imparted to a surface atom is not sufficient to cause desorption, the enhanced vibrational motion could lead to increased surface diffusion.

The removal of adatoms when the surface is irradiated by laser pulses below the melting threshold was found to be site selective, depended strongly on wavelength, and was highly superlinear with respect to excitation laser fluence.[3,45] It was shown that center atoms on Si(111)-(7×7) have higher probability for desorption than corner atoms.[45] Also, surface atoms neighboring an adatom-vacancy pair are more likely to be removed. Preferential bond rupture nearest to pre-existing vacancies was also observed on the Si(111) surface.[6,7] Selective removal of the topmost layer was also shown for Si(100)-(2×1).[46] In this case, localized electronic states at defects, such as vacancies, on the reconstructed surface are believed to be responsible for this selective layer removal.

The process that causes the observed effect of laser irradiation of the substrate must be electronic in nature. A possible scenario involves electron-hole generation in the substrate followed by hole diffusion to the surface and THL.[40] Yu and Tanimura[43] investigated the laser-induced desorption of Si adatoms on Si(100)-(2×1) when the surface is excited by 2.48 eV laser pulses. Their results show that electronic excitation causes desorption of Si atoms from a certain adatom configuration. The desorption yield was superlinearly dependent on the laser fluence and, therefore, was consistent with the THL model. More importantly, desorption yields with successive laser pulses indicated that the adatom configuration that was reactive to desorption transformed by laser excitation into a different form that is less susceptible to desorption. That work led to the conclusion that surface electronic excitation can be a possible method to reduce surface defects.[47,48] Bulk valance excitation of Si(111)-(2×1) using 1064 nm laser pulses was shown to result in a surface vacancy formation at preferential sites near existing surface vacancies.[7] The fluence dependence of the rate of surface vacancy generation and the more effective vacancy site generation for n-doped surfaces were consistent with the THL model. An important point is that the results indicate that free holes are more effectively trapped at surface-defect sites. This suggests that substrate excitation during deposition causes hole localization preferentially at adatom sites.

For 1064 nm photons, Si has an absorption coefficient of $\sim 11\ \mathrm{cm}^{-1}$ and, therefore, the optical excitation is almost uniform near the surface, resulting in negligible carrier diffusion due to the negligible gradient in carrier density generated near the surface. However, it was suggested that the fast surface recombination can lead to a valence hole density gradient near the surface resulting in hole transport from the bulk to the surface.[31] A laser fluence of $106\ \mathrm{mJ/cm}^2$ results in the generation of a carrier density of $\sim 10^{19}\ \mathrm{cm}^{-3}$. Because of the slow carrier decay, the density of holes at the surface can reach $\sim 10^{19}\ \mathrm{cm}^{-3}$ at the end of the laser pulse. However, Yu *et al.*[49] found that electronic bond breaking on Si(100)-(2×1) is effectively inactive below a photon energy of 1.9 eV, which is explained to be a result of the indirect band gap of Si for which the desorption yield was shown to be extremely low for photon energies up to ~1 eV above the band gap. An exception to this observation was on Si(111)-(2×1) which has a surface with strong bond ionicity and differs significantly from the Si(100)-(2×1) surface.[7] Therefore, electronic excitation of the Si(100)-(2×1) substrate and THL at its surface is unlikely to be the mechanism driving epitaxial growth of Ge.

Eaglesham *et al.*[50] showed the existence of a limiting thickness h_{epi}, which depends on the growth rate and temperature, beyond which epitaxy becomes amorphous. The possibility of epitaxial growth of Ge on Si by MBE was shown to occur at a temperature between 50 and 150 °C for h_{epi} of 30 Å and 200 Å, respectively, for a growth rate of $0.2\ \text{Å}\ \mathrm{s}^{-1}$.[51] The rate of deposition affects h_{epi}, which was shown to be reduced to 50 Å at 150 °C when the rate of deposition was increased to $1.7\ \text{Å}\ \mathrm{s}^{-1}$. In the present experiment, each laser pulse with energy density of $5\ \mathrm{J/cm}^2$ deposits ~0.003 ML/pulse ($\sim 1.7\times 10^{12}\ \mathrm{atoms/cm}^2$ per pulse, 1 ML Ge(100) $\sim 6.23\times 10^{14}\ \mathrm{atoms/cm}^2$). It was shown that the laser plasma plume expands very rapidly ($\sim 10^6\ \mathrm{cm/s}$) perpendicular to the ablated surface.[52] The plume expansion results in a plume width of around several microseconds at a 10 Hz repetition rate.[53–56] This results in an instantaneous deposition rate in the 100 s of $\text{Å}\ \mathrm{s}^{-1}$. Nikiforov *et al.*[57] investigated the limiting thickness for Ge growth on Si(100) by using RHEED. In their work, they assumed that the maximum spot intensity corresponds to the maximum epitaxial layer thickness. In Fig. 3, the maximum RHEED spot intensity during Ge growth was reached at ~4 ML, and beyond that thickness, the intensity started to decrease until it completely disappeared. Therefore, although the process of THL on the Si(100)-(2×1) surface is suppressed at the 1064 nm excitation wavelength, for our experiment at 250 °C, epitaxial formation of the wetting layer still occurs up to ~4 ML.

Once the Ge wetting layer is formed, THL can occur on the Ge surface. At 250 °C, the indirect Ge energy band gap is 0.57 eV and Ge has a direct band gap at 0.7 eV. The absorption coefficient of 1064 nm in Ge is $1.6\times 10^4\ \mathrm{cm}^{-1}$, leading to significantly higher electron-hole generation in the Ge wetting layer than the Si substrate. The hole density of germanium due to absorption of the laser pulse is $\sim 10^{23}\ \mathrm{cm}^{-3}$. The surface hole density depends on many parameters that include surface recombination and diffusion across the Si/Ge interface. We are not aware of any studies done on electronic bond breaking of electronically excited Ge surfaces. However, the THL mechanism, followed by the phonon-kick, is applicable to semiconductors in general. En-

ergetically, this mechanism could be effective on Ge surfaces. For surface bond breaking, the phonon-kick has to transfer enough energy to the top atom along the bond direction to break that bond. If that energy transfer is not sufficient for bond breaking, then, the atom will have a vibrational excitation that can lead to surface hopping. Within the experimental error, we have observed no change in the monolayer coverage for Ge on Si with laser excitation.

Therefore, THL on the Ge surface can lead to selective energy transfer to the Ge atoms that landed on the surface from the PLD plume since these atoms constitute a defect site. The energy that is preferentially given to these adsorbed atoms can result in their hopping to settle epitaxially on the surface.

Previous picosecond time-resolved RHEED studies of excitation of the three low-index surfaces of Ge with 1064 nm, 100 ps laser pulses have conclusively shown that the surface temperature behaves as expected from a simple heat diffusion model.[58–61] This rules out an electronic mechanism that transfers energy to surface atoms causing heating above that expected from simple laser absorption in the skin depth followed by heat diffusion. However, we point out that RHEED probes surface atoms over a very large area. The mechanism we are proposing for enhanced surface hopping of the adsorbed Ge atoms is preferential to the adsorbed atoms which is only a very small coverage. Therefore, such preferential enhancement of surface hopping of the adsorbed atoms would not be sufficient to allow it to be detected through RHEED observation of the transient Debye–Waller factor.

Charge transfer from the substrate to the adsorbate or vice versa during thin film growth has been reported to affect the film quality and that atoms may gain vibrational energy because of a charge transfer process.[62–64] Charge transfer interactions are believed to be important and can occur at the interface of a Si substrate.[65] Photoinduced charge transfer between the Ge atoms and Si substrate or the Ge wetting layer may affect the nucleation by increasing the vibrational energy of surface atoms, causing an increase in the surface diffusion. The low photon energy used in the present study, with only ~0.05 eV excess energy above the Si band gap at 300 K and, makes this process ineffective for a Si surface. A possible role of charge transfer between the Ge surface and the Ge adatoms cannot be ruled out at the present time.

3. Enhanced effective surface diffusion

Direct laser heating can be ruled out as the mechanism causing the modification of Ge QD growth on Si(100)-(2×1). However, the exact mechanism responsible is not clear. Enhancement of the effective surface diffusion of adatoms by the excitation laser could be involved. The rate of surface diffusion of atoms D follows an Arrhenius form with temperature and is proportional to the vibrational energy in the reaction coordinate. There are two possible scenarios as stated in Itoh and Stoneham.[2] If surface energy changes due to the electronic excitation, one expects an Arrhenius behavior with a reduced barrier, which can be seen in the form of $\exp[-(E_T-X)/kT]$. However, if this vibrational energy is increased by a fraction of the recombination energy, then one expects an extra term in the denominator as a result of temperature dependence in the form of $\exp[-E_T/(kT+X)]$. In both cases, the surface diffusion coefficient increases.

IV. CONCLUSION

We have studied Ge QD formation on Si(100)-(2×1) with different substrate temperatures and excitation laser energy densities. The excitation laser reduces the epitaxial growth temperature to 250 °C for a 22 ML film. In addition, applying the excitation laser to the substrate during the growth changes the QD morphology and density and improves the uniformity of QDs fabricated at 390 °C. At room temperature, applying the excitation laser during growth decreases the surface roughness although epitaxial growth could not be achieved. We have ruled out thermal effects and some of the desorption models. Although further studies are needed to elucidate the mechanism involved, a purely electronic mechanism of enhanced surface diffusion of Ge atoms is proposed. Further investigation of this electronic modification of thin film growth would benefit from surface diffusion measurement during growth and the use of *in situ* atomic probe microscopy to observe the development of the wetting layer and the QDs and how this is affected by electronic excitation.

Although the effects of electronic excitation on shown for Ge growth on Si(100), the basic principle involved is expected to apply to other semiconductor heteroepitaxy. Achieving low temperature epitaxial growth is an important step for high level integration. Low temperature epitaxy also limits the redistribution of impurities, reduces intermixing in heteroepitaxy, and restricts the generation of defects by thermal stress. The ability to prepare self-assembled QDs with reduced size distribution by electronic excitation is also important for many applications because both the optical and electronic properties of a QD depend on its size. The use of electronic excitation to provide some control on thin film and QD growth could be an important tool in fabricating devices based on self-assembly.

ACKNOWLEDGEMENTS

This material is based upon work supported by the US Department of Energy, Division of Material Science, under Grant No. DE-FG02-97ER45625 and the National Science Foundation under Grant Nos. DMR-9988669 and MRI-0821180.

[1] D. J. Paul, Semicond. Sci. Technol. **19**, R75 (2004).
[2] N. Itoh and A. M. Stoneham, *Materials Modification by Electronic Excitation* (Cambridge University Press, Cambridge, 2001).
[3] K. Tanimura, E. Inami, J. Kanasaki, and W. P. Hess, Phys. Rev. B **74**, 035337 (2006).
[4] Y. Zhang, J. Lian, C. M. Wang, W. Jiang, R. C. Ewing, and W. J. Weber, Phys. Rev. B **72**, 094112 (2005).
[5] J. Kanasaki, K. Iwata, and K. Tanimura, Phys. Rev. Lett. **82**, 644 (1999).
[6] J. Kanasaki, T. Ishida, K. Ishikawa, and K. Tanimura, Phys. Rev. Lett. **80**, 4080 (1998).
[7] E. Inami, K. Ishikawa, and K. Tanimura, Surf. Sci. **540**, L587 (2003).
[8] J. Xu, S. H. Overbury, and J. F. Wendelken, Phys. Rev. B **53**, R4245 (1996).
[9] J. C. Bean, T. T. Sheng, L. C. Feldman, A. T. Fiory, and R. T. Lynch, Appl. Phys. Lett. **44**, 102 (1984).

[10]T. Inoue, Y. Yamamoto, and M. Satoh, J. Vac. Sci. Technol. A **19**, 275 (2001).
[11]W. Ensinger, Nucl. Instrum. Methods Phys. Res. B **127–128**, 796 (1997).
[12]A. Izumi, K. Tsutsui, and S. Furukawa, J. Appl. Phys. **75**, 2307 (1994).
[13]D.-Y. Kim, K.-C. Lee, and C. Lee, J. Korean Phys. Soc. **44**, 341 (2004).
[14]V. A. Fedotov, K. F. MacDonald, N. I. Zheludev, and V. I. Emel'yanov, J. Appl. Phys. **93**, 3540 (2003).
[15]A. V. Dvurechenskii, V. A. Zinov'ev, and Z. V. Smagina, JETP Lett. **74**, 267 (2001).
[16]V. A. Volodin, A. V. Yakimov, A. V. Dvurechenskiĭ, M. D. Efremov, I. Nikiforov, E. I. Gatskevich, G. D. Ivlev, and G. Y. Mikhalev, Semiconductors **40**, 202 (2006).
[17]W. Hoheisel, M. Vollmer, and F. Trager, Phys. Rev. B **48**, 17463 (1993).
[18]I. Lee, T. A. Callcott, and E. T. Arakawa, Phys. Rev. B **47**, 6661 (1993).
[19]Z. Wu, Phys. Lett. A **131**, 486 (1988).
[20]M. S. Hegazy and H. E. Elsayed-Ali, J. Appl. Phys. **104**, 124302 (2008).
[21]A. V. Dvurechenskii, J. V. Smagina, R. Groetzschel, V. A. Zinovyev, V. A. Armbrister, P. L. Novikov, S. A. Teys, and A. K. Gutakovskii, Surf. Coat. Technol. **196**, 25 (2005).
[22]C. Hernandez, Y. Campidelli, D. Simon, D. Bensahel, I. Sagnes, G. Patriarche, P. Boucaud, and S. Sauvage, J. Appl. Phys. **86**, 1145 (1999).
[23]Z. M. Zhang, L. M. Hanssen, and R. U. Datla, Infrared Phys. Technol. **37**, 539 (1996).
[24]E. Inami and K. Tanimura, Surf. Sci. **603**, L63 (2009).
[25]Y. J. Chabal, S. B. Christman, E. E. Chaban, and M. T. Yin, J. Vac. Sci. Technol. A **1**, 1241 (1983).
[26]W. Mönch, P. Koke, and S. J. Krueger, J. Vac. Sci. Technol. **19**, 313 (1981).
[27]K. Tanimura and J. Kanasaki, J. Phys.: Condens. Matter **18**, S1479 (2006).
[28]I. W. Boyd, S. C. Moss, T. F. Howson, and L. J. Willis, Appl. Phys. Lett. **45**, 80 (1984).
[29]D. Srivastava and B. J. Garrison, Phys. Rev. B **46**, 1472 (1992).
[30]J. A. Misewich, T. F. Heinz, and D. M. Newns, Phys. Rev. Lett. **68**, 3737 (1992).
[31]H. M. van Driel, Phys. Rev. B **35**, 8166 (1987).
[32]K. G. Svantesson and N. G. Nilsson, J. Phys. C **12**, 3837 (1979).
[33]G. Betz and P. Varga, *Desorption Induced by Electronic Transitions-DIET IV* (Springer, New York, 1990).
[34]M. L. Knotek and P. J. Feibelman, Phys. Rev. Lett. **40**, 964 (1978).
[35]D. Menzel and R. Gomer, J. Chem. Phys. **41**, 3311 (1964).
[36]P. A. Redhead, Can. J. Phys. **42**, 886 (1964).
[37]J. A. Bearden and A. F. Burr, Rev. Mod. Phys. **39**, 125 (1967).
[38]J. Kanasaki, A. Okano, K. Ishikawa, Y. Nakai, and N. Itoh, Nucl. Instrum. Methods Phys. Res. B **101**, 93 (1995).
[39]E. Inami and K. Tanimura, Phys. Rev. B **76**, 035311 (2007).
[40]H. Sumi, Surf. Sci. **248**, 382 (1991).
[41]J. Kanasaki, M. Nakamura, K. Ishikawa, and K. Tanimura, Phys. Rev. Lett. **89**, 257601 (2002).
[42]P. W. Anderson, Phys. Rev. Lett. **34**, 953 (1975).
[43]I.-K. Yu and K. Tanimura, Solid State Commun. **101**, 429 (1997).
[44]J. Kanasaki, K. Katoh, Y. Imanishi, and K. Tanimura, Appl. Phys. A: Mater. Sci. Process. **79**, 865 (2004).
[45]K. Ishikawa, J. Kanasaki, K. Tanimura, and Y. Nakai, Solid State Commun. **98**, 913 (1996).
[46]N. Itoh, J. Kanasaki, and J. Xu, Prog. Surf. Sci. **61**, 1 (1999).
[47]N. Itoh, K. Hattori, Y. Nakai, J. Kanasaki, A. Okano, C. K. Ong, and G. S. Khoo, Appl. Phys. Lett. **60**, 3271 (1992).
[48]K. S. Khoo, C. K. Ong, and N. Itoh, J. Phys.: Condens. Matter **5**, 1187 (1993).
[49]I.-K. Yu, J. Kanasaki, A. Okano, Y. Nakai, and N. Itoh, J. Phys.: Condens. Matter **8**, 1475 (1996).
[50]D. J. Eaglesham, H.-J. Gossmann, and M. Cerullo, Phys. Rev. Lett. **65**, 1227 (1990).
[51]D. J. Eaglesham and M. Cerullo, Appl. Phys. Lett. **58**, 2276 (1991).
[52]M. Capitelli, A. Casavola, G. Colonna, and A. De Giacomo, Spectrochim. Acta, Part B **59**, 271 (2004).
[53]M. Frumar, B. Frumarova, P. Nemec, T. Wagner, J. Jedelsky, and M. Hrdlicka, J. Non-Cryst. Solids **352**, 544 (2006).
[54]S. Amoruso, R. Bruzzese, N. Spinelli, and R. Velotta, J. Phys. B **32**, R131 (1999).
[55]P. Ohresser, J. Shen, J. Barthel, M. Zheng, Ch. V. Mohan, M. Klaua, and J. Kirschner, Phys. Rev. B **59**, 3696 (1999).
[56]R. Eason, *Pulsed Laser Deposition of Thin Films: Applications-Led Growth of Functional Materials* (Wiley, New York, 2007).
[57]A. I. Nikiforov, B. Z. Kanter, and O. P. Pchelyakov, Thin Solid Films **336**, 179 (1998).
[58]X. Zeng and H. E. Elsayed-Ali, Surf. Sci. **497**, 373 (2002).
[59]X. Zeng and H. E. Elsayed-Ali, Phys. Rev. B **64**, 085410 (2001).
[60]X. Zeng, B. Lin, I. El-Kholy, and H. E. Elsayed-Ali, Phys. Rev. B **59**, 14907 (1999).
[61]X. Zeng, B. Lin, I. El-Kholy, and H. E. Elsayed-Ali, Surf. Sci. **439**, 95 (1999).
[62]S. Sánchez-Cortés and J. V. García-Ramos, Langmuir **16**, 764 (2000).
[63]N. M. Hwang and D. Y. Kim, Int. Mater. Rev. **49**, 171 (2004).
[64]K. Katayama, K. Shibamoto, and T. Sawada, Chem. Phys. Lett. **345**, 265 (2001).
[65]R. Ruiz, D. Choudhary, B. Nickel, T. Toccoli, K.-C. Chang, A. C. Mayer, P. Clancy, J. M. Blakely, R. L. Headrick, S. Iannotta, and G. G. Malliaras, Chem. Mater. **16**, 4497 (2004).